Theoretical and Applied Fracture Mechanics 119 (2022) 103360

Contents lists available at ScienceDirect

Theoretical and Applied Fracture Mechanics

journal homepage: www.elsevier.com/locate/tafmec

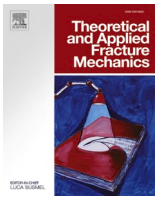

Effects of natural aging and variable loading on very high cycle fatigue behavior of a bearing steel GCr15

Gen Li [a], Lei Ke [b], Wenjie Peng [c], Xuechong Ren [b,*], Chengqi Sun [a,d,*]

[a] State Key Laboratory of Nonlinear Mechanics, Institute of Mechanics, Chinese Academy of Sciences, Beijing 100190, China
[b] National Center for Materials Service Safety, University of Science and Technology Beijing, Beijing 100083, China
[c] Baosteel Central Research Institute, Wuhan 430080, China
[d] School of Engineering Science, University of Chinese Academy of Sciences, Beijing 100049, China

ARTICLE INFO

Keywords:
GCr15
High strength steel
Natural aging
Variable amplitude loading
Very high cycle fatigue
Crack initiation

ABSTRACT

Natural aging and variable amplitude loading are very common for structural parts subjected to fatigue loading. In this paper, ultrasonic frequency fatigue tests without intermittence were conducted to investigate the effects of natural aging and variable amplitude loading on very high cycle fatigue (VHCF) behavior of a high strength steel GCr15. It was shown that a natural aging of 10000 h prolonged the fatigue life of GCr15 steel in VHCF regime. The reason was that more granular carbides precipitated in the microstructure after the natural aging, and they strengthened the fatigue resistance of the material. The natural aging had no influence on the characteristics of the crack initiation and early growth region of GCr15 steel in VHCF regime. The effect of low loading in variable amplitude on fatigue life was related to its loading sequence, loading cycles and stress level. Under step loadings, the low loading with a number of cycles could reduce the fatigue life. The high loading in variable amplitude with a small number of cycles accelerated the crack initiation and growth. It could also change the fatigue failure mechanism to the one dominated by high loading.

1. Introduction

With the rapid development of the modern industrial technology, in fields of aerospace, automotive, high-speed rail and so on, some components need to endure up to 10^7-10^{10} cyclic loadings in service. Therefore, very high cycle fatigue (VHCF, $>10^7$ cycles) behavior of metallic materials has drawn great attention in recent decades [1–5]. In particular, the application of ultrasonic frequency fatigue testing technique enormously saves the time and the cost of fatigue test, which stimulates the development in this field.

Bearing steels are important metallic materials used in structural parts, which could work under cyclic loading. The effects of some factors on VHCF behaviors of these steels have been investigated, including stress ratio, loading frequency, thermal aging and so on [6–9]. In actual engineering applications, the materials and structural parts are not always used immediately after production, namely they might be stored for a period before their application. Accordingly, natural aging would happen in this period, and its effect needs to be clarified. However, to the author's knowledge, the studies for the effect of natural aging on the fatigue behavior of bearing steels is still lacking. In existing studies, the natural-aging effect on the mechanical behaviors of different steels was varied. Botvina et al. [10] tested a low carbon steel after storage of 15 years at room temperature and found that its fatigue strength decreased significantly after long-term natural aging due to corrosion and hydrogen penetration at local regions. Chang [11] and Zamani et al. [12] studied short-term natural-aging effect on low carbon dual phase steel at room temperature and found that the natural aging enhanced the tensile strength and the hardness of the material. Their results indicated that the ferrite phase became supersaturated due to carbon and fine precipitates formed in ferrite grains. The discrepancy and limited understanding of the natural-aging effect for the different materials make it necessary for the investigation of the natural-aging effect on bearing steels.

Moreover, variable amplitude fatigue loading is very common for metallic components in service, such as the axles of high-speed trains. It is of great significance to investigate the fatigue behavior of steels under variable amplitude loading [13–18]. For example, Mayer [16] studied a low carbon steel and indicated that the low loading could reduce or

* Corresponding authors at: State Key Laboratory of Nonlinear Mechanics, Institute of Mechanics, Chinese Academy of Sciences, Beijing 100190, China (Chengqi Sun).
E-mail addresses: Xcren@ustb.edu.cn (X. Ren), scq@lnm.imech.ac.cn (C. Sun).

https://doi.org/10.1016/j.tafmec.2022.103360
Received 11 January 2022; Received in revised form 8 April 2022; Accepted 13 April 2022
Available online 16 April 2022

Table 1
Chemical composition of GCr15 steel (wt%).

C	Cr	Mn	Si	P	S	Fe
1.00	1.52	0.31	0.21	0.0086	0.016	balance

Table 2
Loading sequences of the present study.

	Effect of natural aging	Effect of low loading				Effect of high loading	
	(Constant loading)	CA-L	VA-L1*	VA-L2	VA-L3	CA-H	VA-H
$\sigma_{a,1}$ (MPa)	900	850	850	850	850	800	800
$\sigma_{a,2}$ (MPa)	–	–	400	400	600	–	1100

* The two-step loading sequence was repeated for five times, then the constant amplitude fatigue test was carried out at $\sigma_a = 850$ MPa until the specimen failed.

prolong the fatigue life under two-step variable amplitude axial loading. This behavior depended on the high loading in the variable amplitude loading. If the high stress amplitude was more than 13% above the constant amplitude endurance limit at 10^9 cycles, the low loading cycles shortened the fatigue life, and vice versa. Mayer et al. [15] investigated the VHCF behavior of the 100Cr6 steel under variable amplitude loading by a cumulative frequency distribution of stress amplitudes. It was found that if the maximum stress amplitude in the variable sequence was close to the fatigue limit under the constant amplitude loading, the crack initiation from interior inclusions occurred earlier. The facets formed under variable amplitude loading were larger than those under constant amplitude loading. Due to the specific fatigue behavior under variable amplitude loading in VHCF regime, fully understanding the effect of variable loading on the VHCF behavior of bearing steels is meaningful and valuable.

The current work aimed to study the effects of natural aging and variable amplitude loading on the VHCF behavior of a bearing steel GCr15 by using ultrasonic frequency fatigue test. For the natural-aging effect, two groups of fatigue tests were conducted with a time gap of 10000 h (14 months). The microstructures before and after natural aging were examined by an optical microscope. For the variable amplitude loading, the effects of low and high loadings on the VHCF behavior were investigated. The fatigue life and failure modes of these specimens were examined and discussed in detail. The crack initiation mechanism under different loading sequences was also analyzed based on the scanning electron microscope (SEM) observation of the fatigue fracture surface. The results could provide valuable references for the engineering application of GCr15 steel and other high strength steels subjected to VHCF loadings.

2. Materials and experimental procedures

2.1. Materials and specimens

The material used in this paper was a high carbon chromium bearing steel (GCr15), and its chemical composition is shown in Table 1. The specimens were machined out from a steel bar and then were heated at 850 ℃ in vacuum furnace for 1 h, followed by oil-quenched and tempered at 200 ℃ in air for 2 h. The heat-treated specimens owned the tensile strength of 2375 MPa and the microhardness of 812 HV.

2.2. Testing methods

The fatigue tests of the GCr15 specimens were conducted on an ultrasonic fatigue test machine (Shimadzu USF-2000A) at a resonance frequency of 20 kHz and a stress ratio (R) of −1 at room temperature in air. The testing system was controlled by the displacement, and the stress amplitude was calibrated through the displacement at the end of the specimen [19]. The continuous loading was used in all the experiments, and the specimens were cooled down by compressive air during the tests. Before fatigue tests, the surfaces of all the specimens were polished to mirror finish to eliminate the effect of machining scratches.

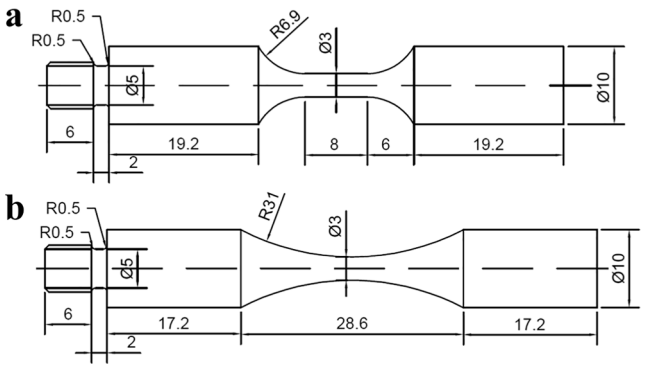

Fig. 1. Geometries of specimens for ultrasonic fatigue tests (in mm): (a) specimen for studying the effects of natural aging and high loading, (b) specimen for studying the effect of low loading.

The fatigue tests in the study included three parts, as shown in Table 2. The first part was the study for natural-aging effect and the heat-treated specimens were tested in two groups, viz. the initial specimens and the specimens after a natural aging of 10000 h. The test results of the initial specimens were referred to Ref. [2]. Due to an interest of comparison of the fatigue behavior in VHCF regime, specimens were tested under a stress amplitude of 900 MPa after natural aging. The geometry of the specimen for the study of natural-aging effect is shown in Fig. 1(a). The hardness was measured by a microhardness tester with a load of 500 gf and holding time of 10 s to investigate the hardness variation due to the natural aging.

The second part was the study for the effect of low loading in variable amplitude loading on VHCF behavior. The geometry of the specimen is shown in Fig. 1(b). The loading sequences were designed due to the consideration that if the fatigue damage produced by the target loading was large enough, the subsequent low loading in the variable amplitude loading should promote the fatigue damage or crack growth in the crack initiation and early growth stage and reduce the VHCF life. Four different loading sequences were conducted in the fatigue tests to study the effect of low loading in variable amplitude loading. The details are given as follows:

i) Constant amplitude loading (CA-L): the stress amplitude was $\sigma_{a,1} = 850$ MPa.
ii) Variable amplitude loading 1 (VA-L1): the fatigue test started from the target stress amplitude $\sigma_{a,1} = 850$ MPa with 10^6 cycles, and then was followed by the low stress amplitude $\sigma_{a,2} = 400$ MPa with 10^7 cycles. If the specimen did not fail after the two-step loading repeated for five times, the constant amplitude fatigue test was carried out at $\sigma_a = 850$ MPa until it failed.
iii) Variable amplitude loading 2 (VA-L2): the fatigue test started from the target stress amplitude $\sigma_{a,1} = 850$ MPa with 10^5 cycles, and then was followed by the low stress amplitude $\sigma_{a,2} = 400$ MPa with 10^5 cycles.
iv) Variable amplitude loading 3 (VA-L3): the fatigue test started from the target stress amplitude $\sigma_{a,1} = 850$ MPa with 10^5 cycles, and then was followed by the low stress amplitude $\sigma_{a,2} = 600$ MPa with 10^5 cycles.

The study for the effect of high loading on the VHCF behavior was the third part. The geometry of the specimen is shown in Fig. 1(a). Two loading sequences were conducted in this part:

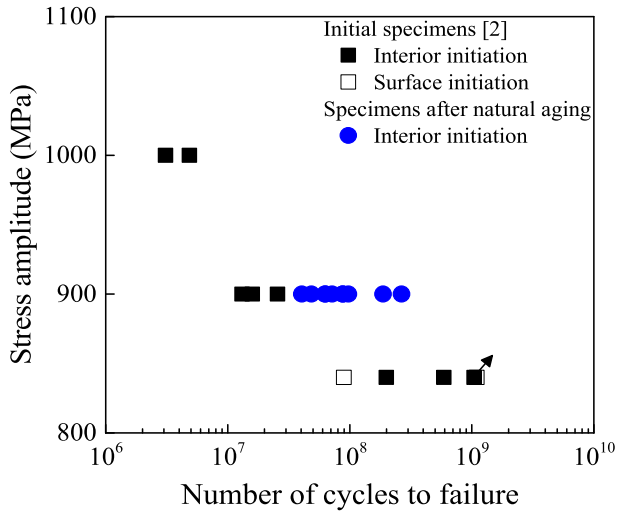

Fig. 2. Stress amplitude versus fatigue life. The arrow denotes the run-out specimen.

i) Constant amplitude loading (CA-H): the stress amplitude was $\sigma_{a,1} =$ 800 MPa.
ii) Variable amplitude loading (VA-H): the fatigue test started from the target stress amplitude $\sigma_{a,1} = 800$ MPa with 2×10^6 cycles, and then was followed by the high stress amplitude $\sigma_{a,2} = 1100$ MPa with 6×10^3 cycles.

The microstructure of the initial specimens and the specimens after natural aging was observed by an optical microscope. All fatigue fracture surfaces of the failed specimens were observed by the SEM. The sizes of the crack origin and the fine granular area (FGA, i.e., crack initiation and early growth region) were measured by Image-Pro Plus (IPP) software.

3. Results and discussion

3.1. Effect of natural aging

The stress amplitude and fatigue life of the initial specimens and the specimens after natural aging are shown in Fig. 2. It was found that the specimens after a natural-aging period of 10000 h presented longer fatigue lives under the stress amplitude of 900 MPa. The fatigue lives of the aged specimens ranged from 4.0×10^7 to 2.6×10^8 cycles, and those of the initial specimens ranged from 1.3×10^7 to 2.6×10^7 cycles. These results suggested that the natural aging was beneficial for the fatigue performance of GCr15 steel in VHCF regime. However, Botvina et al. [10] reported negative effect of natural aging on the fatigue strength of a low carbon steel. It was attributed to corrosion and hydrogen penetration during the storage of 15 years (>130000 h).

To study the mechanism of natural-aging effect on the fatigue life, the microstructures of the initial specimens and the specimens after natural aging were compared firstly. As shown in Fig. 3(a), the microstructure of the initial specimens was tempered martensite with fine granular carbides. However, more granular carbides precipitated in the microstructure after natural aging in Fig. 3(b). This was due to the high content of solute carbon in the martensite in the initial specimens, which resulted in the precipitation of granular carbides after the natural aging. The hardness of the initial specimens and the specimens after natural aging was also compared, which increased from 812 HV to 944 HV. This phenomenon was consistent with the precipitation hardening effect on metallic materials in literature [11,12,20]. The material was strengthened after natural aging, and it restrained crack nucleation and growth, and prolonged the fatigue life of the specimens.

The fatigue fracture surfaces of the tested specimens were then observed by SEM to investigate the effect of natural aging on the mechanism of crack initiation and early growth. Both the initial specimens and the specimens after natural aging failed from the internal crack initiation with fish-eye and FGA features, which were commonly observed for high strength steels in VHCF regime [2,21]. SEM observation also indicated that the crack origins were due to microstructure inhomogeneity or inclusion for both the initial specimens and the specimens after natural aging. The fatigue fracture surface morphologies of an initial specimen and a specimen after natural aging are shown in Fig. 4(a-1 to a-3) and 4(b-1 to b-3), respectively. For high strength steels, FGA is a characteristic region for crack initiation and early growth [2]. Therefore, the FGA sizes (square root of the FGA area including the projection area of crack origin) of the tested specimens were measured to examine the effect of natural aging on the crack initiation and early growth. The FGA size versus the fatigue life is shown in Fig. 5. It indicated that the FGA sizes of the initial specimens and the specimens after natural aging did not present obvious difference, which varied in a range of 47.2 μm to 56.5 μm. Besides, the crack origin sizes were also measured for the initial specimens and the specimen after natural aging, and they did not show obvious relation with the fatigue life. In this way, the natural aging did not change the characteristics of crack initiation and early growth of the GCr15 steel in VHCF regime.

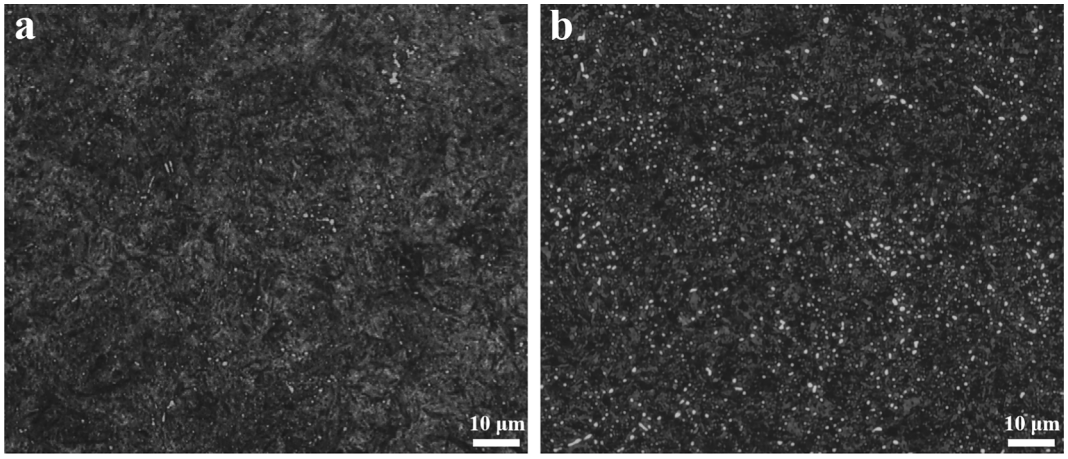

Fig. 3. Microstructure of specimens: (a) initial specimen, (b) specimen after natural aging.

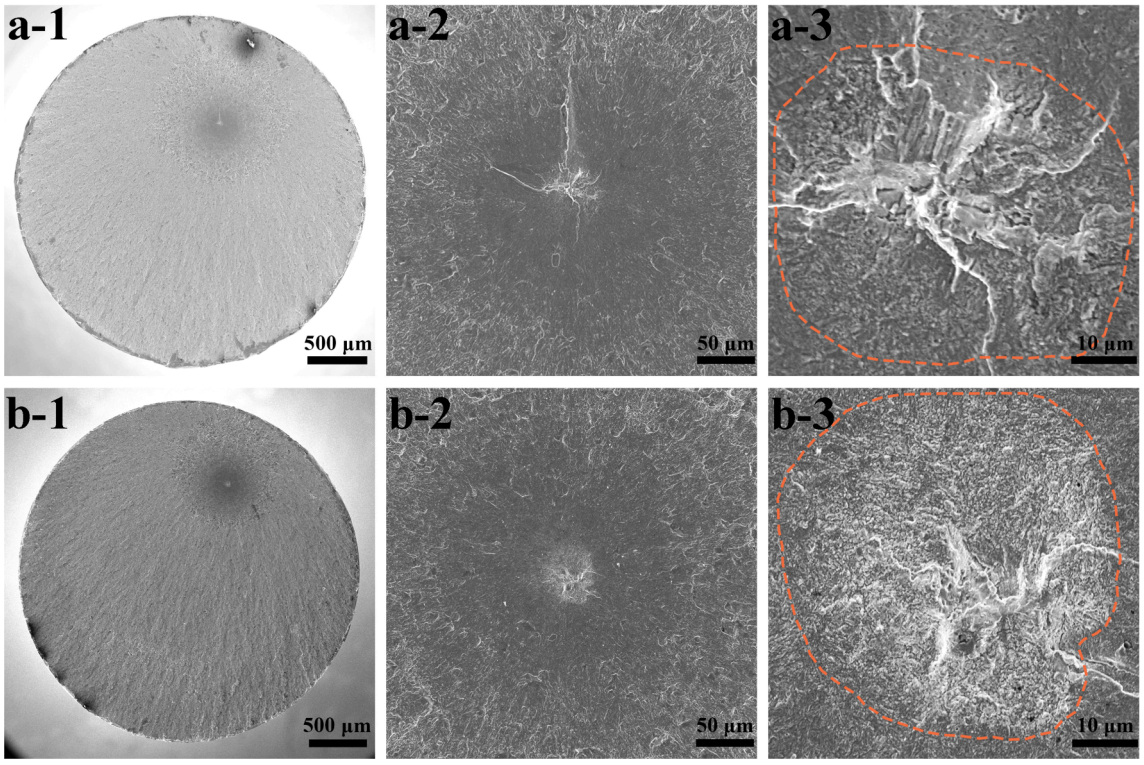

Fig. 4. SEM images of typical fatigue fracture surfaces: (a-1) to (a-3): initial specimen σ_a = 900 MPa, $N_f = 1.3 \times 10^7$; (a-2) and (a-3) are close-ups of the crack initiation and early growth region in (a-1). (b-1) to (b-3): the specimen after natural aging σ_a = 900 MPa, $N_f = 1.9 \times 10^8$; (b-2) and (b-3) are close-ups of the crack initiation and early growth region in (b-1). The regions marked by the dash lines in (a-3) and (b-3) denote the FGA.

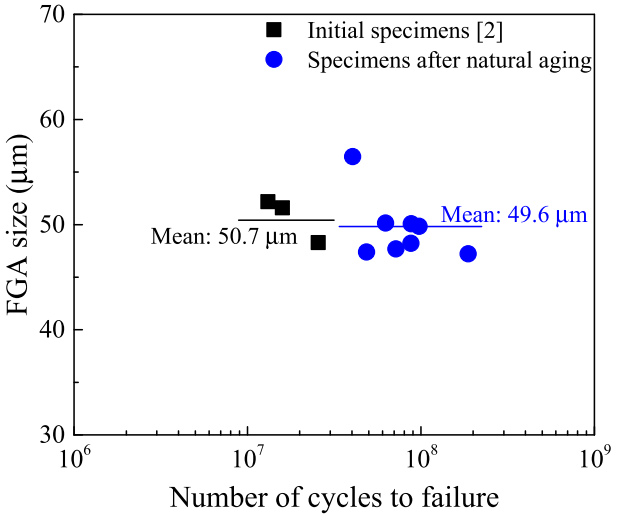

Fig. 5. Comparison of FGA sizes for the initial specimens and the specimens after natural aging tested at 900 MPa.

3.2. *Effect of variable loading*

3.2.1. *Effect of low loading*

Fig. 6 shows the comparison of fatigue life under the constant amplitude and variable amplitude with low loading. The fatigue life in Fig. 6 is the cumulative loading cycles under the target stress amplitude $\sigma_{a,1}$. Detailed fatigue life data under the constant and variable amplitude loadings are shown in Table 3. It is seen from Fig. 6(a) that the scatter of fatigue life data for VA-L1 is almost the same as those for CA-L. The fatigue life data for VA-L2 and VA-L3 seemed to be shorter than those for CA-L as a whole, though the scatter of the fatigue life for VA-L2 and VA-L3 was slightly increased. Considering the scatter of the fatigue life data, survival probability was introduced to further analyze the effect of low loading in variable loading. The fatigue life data in logarithm under each loading sequence were assumed to follow Weibull distribution [22], and the fatigue lives at 50% and 90% survival probabilities were calculated, as shown in Fig. 6(b). It was found that the fatigue lives at 50% survival probability under all the three variable amplitude loading were shorter than that under the constant amplitude loading. Moreover, the fatigue lives at 90% survival probability decreased gradually for VA-L1, VA-L2 and VA-L3. These results indicated that the low stress amplitudes of 400 MPa and 600 MPa in variable amplitude loadings could be detrimental for the fatigue life in terms of the target stress amplitude of 850 MPa (i.e., the cumulative loading cycles at the target stress amplitude), namely the low loading in variable amplitude loading could promote the crack initiation or early growth and reduced the fatigue life. The detailed discussion is given later in this Section.

The fatigue fracture surfaces under CA-L, VA-L1, VA-L2 and VA-L3 were examined by SEM and all of them failed from internal crack initiation with fish-eye and FGA feature, as shown in Fig. 7. The comparison of the fatigue fracture surfaces among the four different loading sequences indicated that the low loading in variable amplitude loading had no obvious influence on the crack initiation and early growth characteristics for the GCr15 steel.

Following the analysis of the fatigue fracture morphology, the sizes of the FGA and the crack origin (i.e., a_{FGA} and a_{Ori}) were measured for the specimens under the four different loading sequences, and they are given in Table 3. The FGA sizes and the mean values with error bars under different loading sequences are plotted in Fig. 8(a). It was seen that the values of the FGA under VA-L2 and VA-L3 tended to be slightly larger than those under CA-L as a whole, and the mean value of FGA under VA-L3 was higher than that under VA-L2. These results indicated that the low loading in variable amplitude loadings could enlarge the FGA size, and this effect could be enhanced with the increase of the low

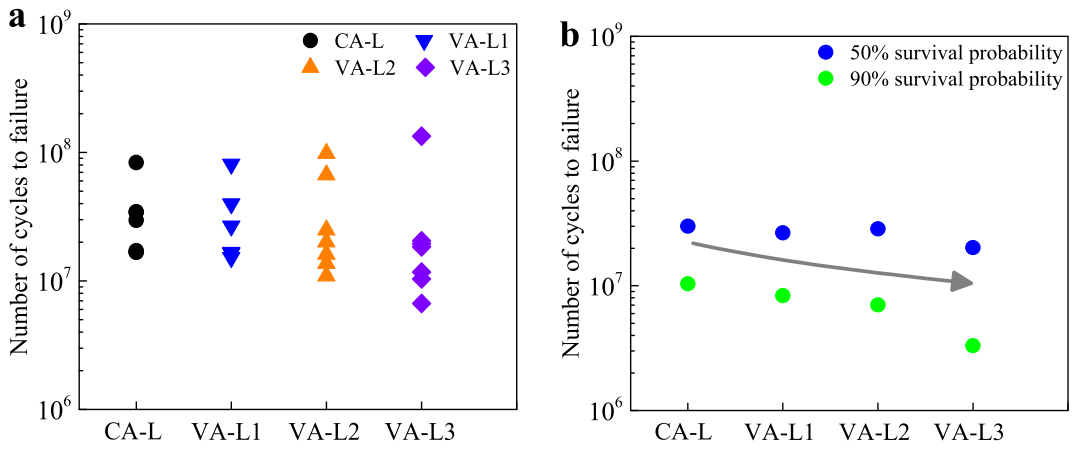

Fig. 6. Comparison of fatigue life under different loading sequences: (a) fatigue life, (b) fatigue life at different survival probabilities.

Table 3
Fatigue life data and sizes of FGA and crack origin under constant and variable amplitude loadings.

Loading sequence	Sample No.	$\sigma_{a,1}$ (MPa)	Cumulative cycles $N_{f,1}$ at $\sigma_{a,1}$	$\sigma_{a,2}$ (MPa)	Cumulative cycles $N_{f,2}$ at $\sigma_{a,2}$	FGA size a_{FGA} (μm)	Size of crack origin a_{Ori} (μm)
CA-L	1	850	1.7×10^7			34.2	14.7
	2	850	3.4×10^7			40.4	20.1
	3	850	1.7×10^7			43.0	12.3
	4	850	8.3×10^7			36.5	28.3
	5	850	3.5×10^7			43.0	16.3
	6	850	1.7×10^7			45.8	20.5
	7	850	3.0×10^7			45.7	17.3
VA-L1	1	850	4.0×10^7	400	5.0×10^7	40.3	15.7
	2	850	1.6×10^7	400	5.0×10^7	40.0	13.2
	3	850	1.6×10^7	400	5.0×10^7	43.1	22.1
	4	850	8.1×10^7	400	5.0×10^7	52.7	37.8
	5	850	1.7×10^7	400	5.0×10^7	40.6	20.2
	6	850	2.7×10^7	400	5.0×10^7	32.7	19.4
	7	850	1.5×10^7	400	5.0×10^7	51.4	25.0
VA-L2	1	850	6.7×10^7	400	6.7×10^7	44.9	22.7
	2	850	2.5×10^7	400	2.5×10^7	50.5	26.7
	3	850	1.6×10^7	400	1.6×10^7	49.6	18.1
	4	850	1.4×10^7	400	1.4×10^7	46.2	13.9
	5	850	2.0×10^7	400	2.0×10^7	45.3	16.9
	6	850	1.1×10^7	400	1.1×10^7	45.3	19.4
	7	850	9.8×10^7	400	9.8×10^7	36.9	12.5
VA-L3	1	850	1.9×10^7	600	1.9×10^7	48.0	19.2
	2	850	1.8×10^7	600	1.8×10^7	46.2	14.1
	3	850	2.1×10^7	600	2.1×10^7	39.1	15.4
	4	850	1.3×10^8	600	1.3×10^8	45.1	2.2
	5	850	1.2×10^7	600	1.2×10^7	44.7	16.9
	6	850	1.0×10^7	600	1.0×10^7	47.2	17.8
	7	850	6.7×10^6	600	6.6×10^6	53.6	19.2

loading under the same loading sequence.

Existing studies have shown that the stress intensity factor range for the crack origin (ΔK_{Ori}) and FGA (ΔK_{FGA}) are important parameters for the crack initiation and early growth of high strength steels in VHCF regime and the equivalent crack growth rate in FGA increases with the higher stress intensity factor range [2,21,23]. This indicated that, in the crack initiation and early growth stage, once the stress intensity factor range for the initiated crack under the low stress amplitude was higher than ΔK_{Ori} under the target stress amplitude, the low stress amplitude would promote the damage development or crack growth comparable with that under target stress amplitude in FGA. Here, to study the effect of low loading on the crack initiation and early growth, the values of ΔK_{Ori} under the target stress amplitude and the values of ΔK_{FGA} under the low stress amplitude were calculated and compared, in which $\Delta K_{Ori} = 0.5\sigma_a \sqrt{\pi a_{Ori}}$ [23,24] and $\Delta K_{FGA} = 0.5\sigma_a \sqrt{\pi a_{FGA}}$ [21]. The data of the ΔK_{Ori} and the ΔK_{FGA} are shown in Fig. 8(b). The values of ΔK_{Ori} under the four different loading sequences were distributed in a range of 1.12 to 4.63 MPa·m$^{1/2}$ and showed a mean value of 3.19 MPa·m$^{1/2}$. As a comparison, the values of ΔK_{FGA} under the low stress amplitude of 600 MPa varied in a range of 3.32 to 3.89 MPa·m$^{1/2}$, which were higher than the mean value of the ΔK_{Ori} and all the values of the ΔK_{Ori} under VA-L3. Therefore, the low stress amplitude of 600 MPa in VA-L3 could drive the damage development or equivalent crack growth in the crack initiation and early growth stage, though at a lower growth rate than that under the target stress amplitude of 850 MPa. Moreover, based on existing studies [2,9,21,23,25,26], the values of ΔK_{FGA} were approximately constants for high strength steels under the constant amplitude loading, namely a lower stress amplitude tended to produce larger FGA. It should be the reason that the specimens under VA-L3 tended to produce larger FGA than those under CA-L. For VA-L2, the values of ΔK_{FGA} under the low stress amplitude of 400 MPa varied between 2.15 MPa·m$^{1/2}$ and 2.52 MPa·m$^{1/2}$, which were within the scatter band of ΔK_{Ori} though they were lower than the mean value of ΔK_{Ori}. The results indicated that the low stress amplitude of 400 MPa could gently aggravate the fatigue

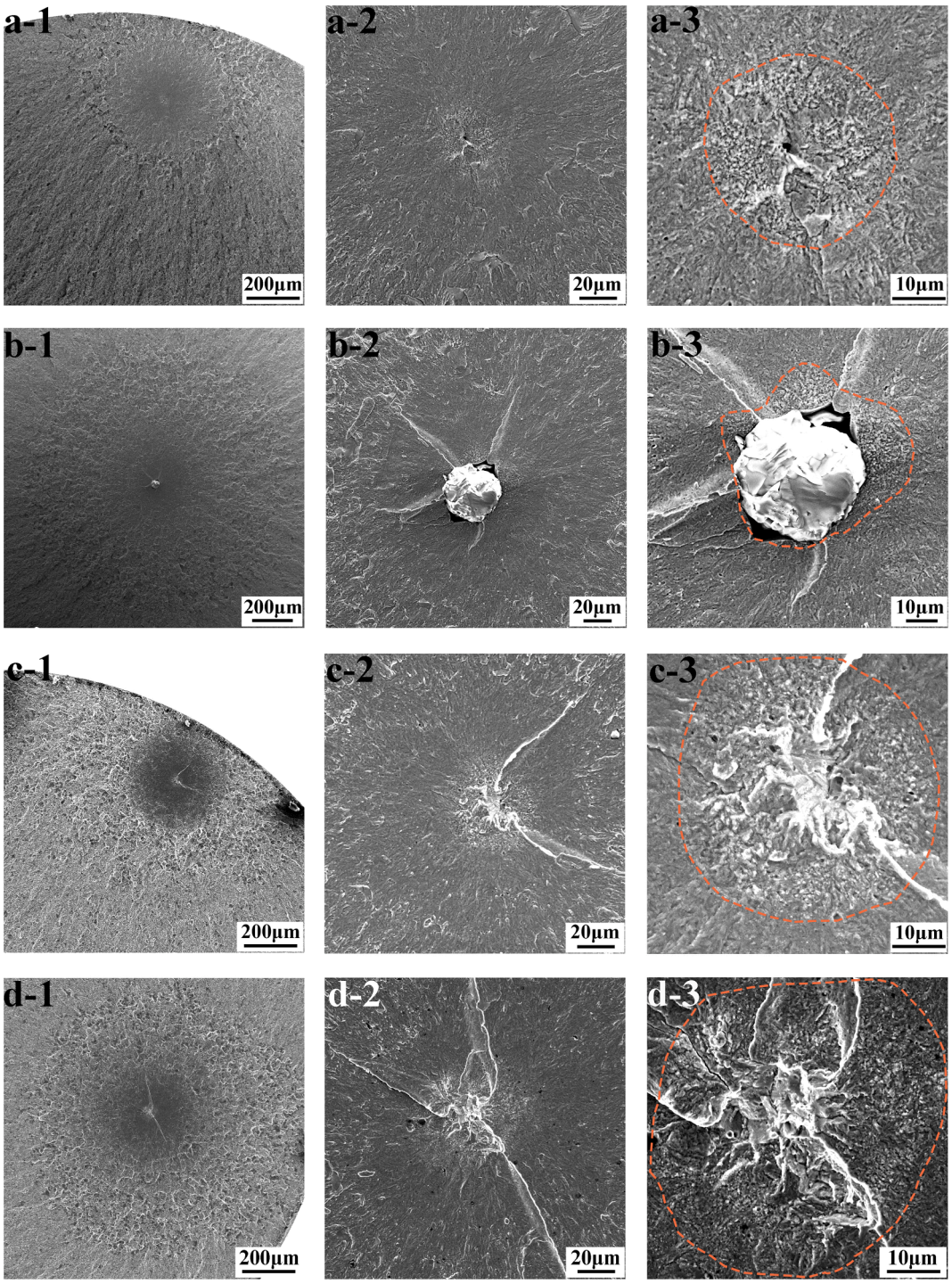

Fig. 7. SEM images of fatigue fracture surface for specimens under different loading sequences: (a-1) to (a-3): CA-L, $\sigma_{a,1} = 850$ MPa, $N_{f,1} = 1.7 \times 10^7$; (a-2) and (a-3) are close-ups of the crack initiation and early growth region in (a-1) and (a-2), respectively. (b-1) to (b-3): VA-L1, $\sigma_{a,1} = 850$ MPa, $N_{f,1} = 8.1 \times 10^7$; (b-2) and (b-3) are close-ups of the crack initiation and early growth region in (b-1) and (b-2), respectively. (c-1) to (c-3): VA-L2, $\sigma_{a,1} = 850$ MPa, $N_{f,1} = 1.1 \times 10^7$, (c-2) and (c-3) are close-ups of the crack initiation and early growth region in (c-1) and (c-2), respectively; (d-1) to (d-3): VA-L3, $\sigma_{a,1} = 850$ MPa, $N_{f,1} = 6.7 \times 10^6$, (d-2) and (d-3) are close-ups of the crack initiation and early growth region in (d-1) and (d-2), respectively. The regions marked by the dash line in (a-3) to (d-3) denote the FGA.

damage in the microstructure or cause the equivalent crack growth in the crack initiation and early growth stage. Therefore, the FGA sizes formed under VA-L2 tended to be slightly larger than those under CA-L, but smaller than those under VA-L3, which agree with the experimental data in Fig. 8(a). The higher low stress amplitude in VA-L3 than that in VA-L2 led to the earlier formation of the crack initiation and early growth region for the specimens, which resulted in the lower fatigue lives at 50% and 90% survival probabilities under VA-L3 than those under VA-L2, as shown in Fig. 6(b).

3.2.2. *Effect of high loading*

Fig. 9 shows the comparison of fatigue lives under the constant amplitude loading CA-H and variable amplitude loading VA-H. The fatigue life is the cumulative loading cycles under the target stress amplitude of 800 MPa. Detailed fatigue life data under CA-H and VA-H are shown in Table 4. For the fatigue tests under CA-H, all the specimens

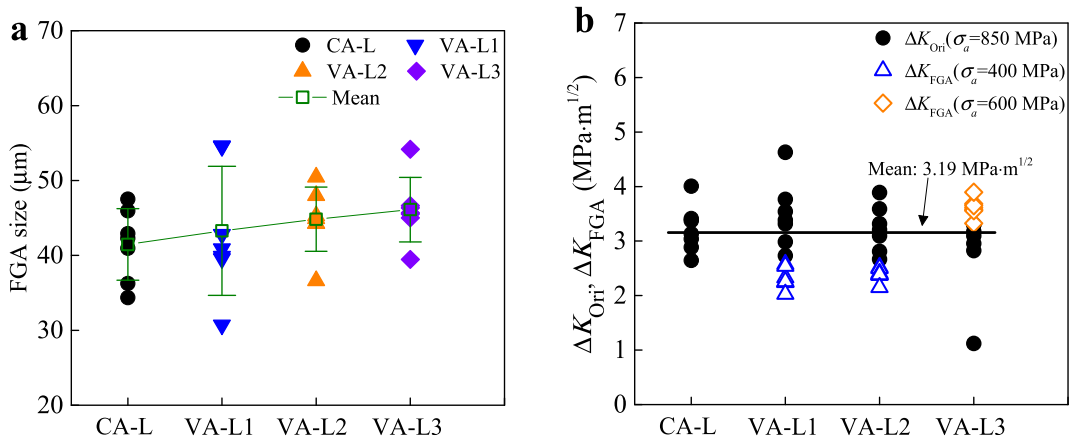

Fig. 8. FGA size, ΔK_{Ori} and ΔK_{FGA} under different loading sequences: (a) FGA sizes, (b) ΔK_{Ori} and ΔK_{FGA}.

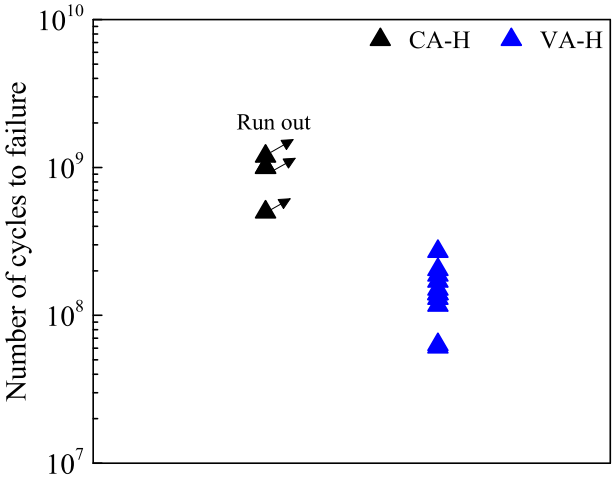

Fig. 9. Comparison of fatigue life between constant and variable amplitude loadings.

Table 4
Fatigue life data and FGA size under constant and variable amplitude loadings.

Loading sequence	Sample No.	$\sigma_{a,1}$ (MPa)	Cumulative cycles $N_{f,1}$ at $\sigma_{a,1}$	$\sigma_{a,2}$ (MPa)	Cumulative cycles $N_{f,2}$ at $\sigma_{a,2}$	FGA size a_{FGA} (μm)
CA-H	1	800	*1.0×10^9			
	2	800	*1.0×10^9			
	3	800	*5.0×10^8			
	4	800	*1.0×10^9			
	5	800	*1.2×10^9			
VA-H	1	800	1.3×10^8	1100	2.6×10^5	65.3
	2	800	1.9×10^8	1100	3.7×10^5	77.1
	3	800	2.7×10^8	1100	5.4×10^5	89.2
	4	800	1.2×10^8	1100	2.3×10^5	35.0
	5	800	6.3×10^7	1100	1.3×10^5	85.7
	6	800	6.1×10^7	1100	1.2×10^5	77.2
	7	800	1.4×10^8	1100	2.7×10^5	72.2
	8	800	2.0×10^8	1100	6.1×10^5	140.8
	9	800	1.7×10^8	1100	5.2×10^5	85.1
	10	800	1.4×10^8	1100	4.1×10^5	81.3
	11	800	1.5×10^8	1100	4.5×10^5	50.2

* It denotes that the specimen did not fail at the associated loading cycles.

did not fail at the loading cycles more than 5×10^8. However, for the fatigue tests under VA-H, the high stress amplitude of 1100 MPa reduced the fatigue life of the specimens in terms of the target stress amplitude to a range of 6.1×10^7 to 2.7×10^8 cycles. This result indicated that the high stress amplitude in the variable amplitude loading, even with a small number of loading cycles, could induce or accelerate the crack initiation and growth, and eventually resulted in the decrease of the fatigue life in terms of the target stress amplitude.

The specimens tested under VA-H all failed from internal crack initiation and some of the fracture surfaces presented "tree-ring" like patterns, as shown in Fig. 10(a) and 10(b). According to the literature [2], the fatigue fracture surface of the GCr15 specimens tested under the constant stress amplitude of 1100 MPa did not presented clear FGA feature but a relatively smooth area around the crack initiation site. Therefore, the fine granular area (rough area) in Fig. 10(b) was produced under the target stress amplitude of 800 MPa and the smooth area between the rough area (the region between R_1 and R_2 in Fig. 10(b)) corresponded to the high stress amplitude of 1100 MPa. It showed the evidence that the high loading in the variable amplitude loading accelerated the formation of crack initiation and early growth region compared with that under CA-H.

Moreover, the FGA sizes under VA-H were measured, and the values are given in Table 4. Here, the FGA size included the smooth area due to the high loading (i.e., the area with a radius of R_3 in Fig. 10(b)). The values of ΔK_{FGA} were calculated and the data versus the fatigue life in terms of the target stress amplitude of 800 MPa are shown in Fig. 11. The values of ΔK_{FGA} for the same specimens tested under different constant stress amplitudes in Ref. [2] are provided for comparison in Fig. 11. The mean value of ΔK_{FGA} under VA-H was 6.18 MPa·m$^{1/2}$, which was higher than that of 5.40 MPa·m$^{1/2}$ under the constant amplitude loadings. It indicated that the variable amplitude loading with high loading moderately increased the value of ΔK_{FGA}. The reason might be that larger plastic zone was created at the crack tip after the high loading in variable amplitude loading. The larger plastic zone in steels usually retarded the crack growth induced by the following low fatigue loading [27–29], which led to the higher ΔK_{FGA} for further crack growth under the target stress amplitude in the specimens.

3.3. Discussion

3.3.1. Effect of low loading

The study in Section 3.2.1 indicated that the low loading (e.g. the stress amplitude with the fatigue life larger than 10^9 cycles) in variable amplitude loadings could reduce the fatigue life under the target stress amplitude (e.g. the stress amplitude with the fatigue life between 10^7 to 10^9 cycles) in VHCF regime. It could be explained as follows. The lifetime of crack initiation and early growth accounted for over 90% of the total fatigue life for high strength steels in VHCF regime [30–32]. During this stage, if the crack or damage region formed under the target stress amplitude was minor and the subsequent low stress amplitude was

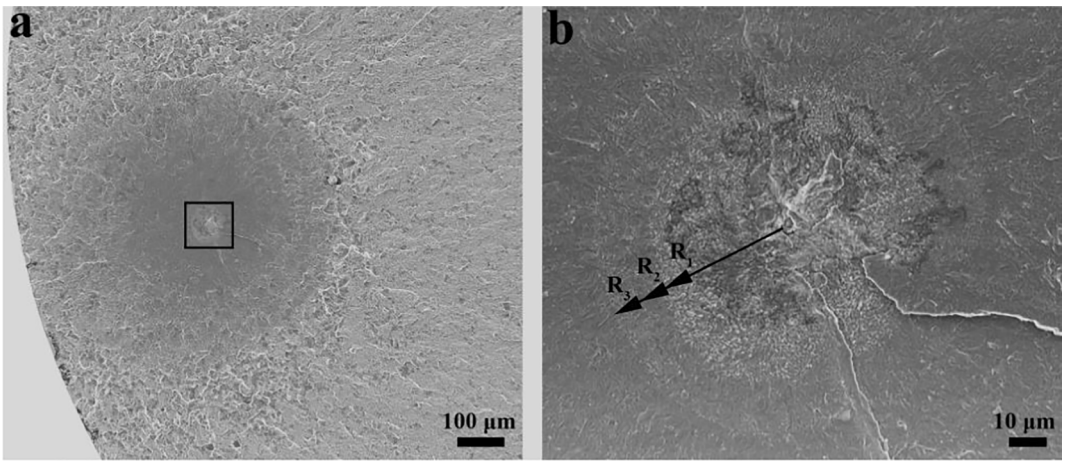

Fig. 10. Fatigue fracture surface morphology of a specimen under VA-H with $N_{f,1} = 2.7 \times 10^8$. (a) Low magnification of the crack initiation and early growth region, (b) Close-up for the rectangular region in (a), in which R_1 and R_3 denote the marks after the sequence of target stress amplitude, R_2 denotes the mark after the sequence of high stress amplitude.

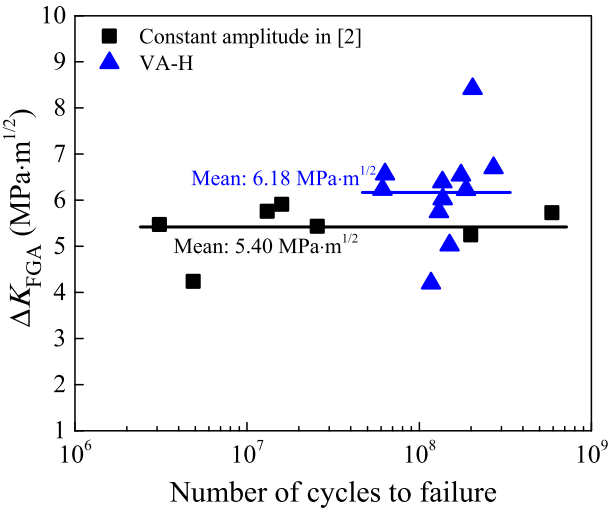

Fig. 11. Values of ΔK_{FGA} versus fatigue life in terms of target stress amplitude under VA-H and fatigue life under different constant amplitude loadings in Ref. [2].

relatively small, or in a small number of loading cycles, the low loading was not able to promote obvious crack growth or damage development. In this way, the effect of the low loading in variable amplitude loading on the fatigue life in terms of the target loading was negligible, such as the fatigue data under VA-L1 in Fig. 6. Once the crack or damage region produced by the target stress amplitude was large enough, the following low loading was able to promote the crack growth or damage development, and finally reduced the fatigue life, as shown in the results of VA-L3 in Fig. 6.

It should be noted that existing results for the same high strength steel have shown that the low loading in variable amplitude loading could improve the fatigue life in VHCF regime [17]. This phenomenon was also found in the fatigue behavior of other steels [33–35]. According to the literature [33,36], the stress amplitude of 75% to 95% of the fatigue limit with a range of 2×10^5 to 4×10^5 cycles at the beginning could obviously strengthen the fatigue performance of steels due to work hardening or micro-plastic deformation. Therefore, the effect of low loading in variable amplitude loading on fatigue life is not only related to the material itself but also related to the loading sequence, loading cycles and stress level.

3.3.2. *Effect of high loading*

The results in Section 3.2.2 indicated that the high loading (e.g. the stress amplitude with high cycle fatigue life) with a small number of cycles in variable amplitude loading was detrimental for the fatigue life in terms of the target stress amplitude in VHCF regime. It was due to that the high loading promoted the crack initiation or fatigue damage in VHCF. For example, the GCr15 specimens did not fail at loading cycles more than 5×10^8 under the constant amplitude loading in Fig. 9. While the specimens failed at much shorter fatigue life than 5×10^8 cycles

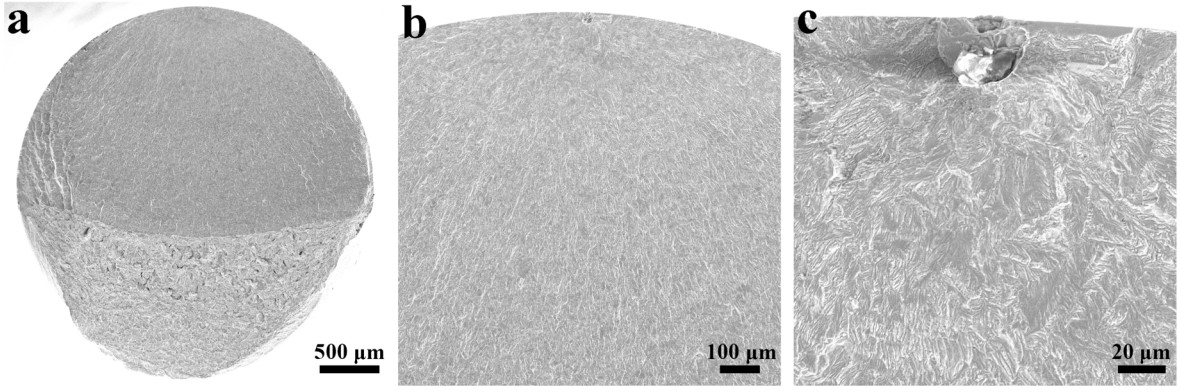

Fig. 12. Fatigue fracture surface of the AISI630 specimen under variable amplitude loading with fatigue life of 1.5×10^7 in terms of the stress amplitude σ_a=450 MPa [21]: (a) whole fracture surface; (b) and (c) are close-ups of the surface crack initiation site in (a) and (b), respectively.

under the variable amplitude loading, and some specimens presented "tree-ring" feature on the fracture surface, as shown in Fig. 10. Since the FGA was not observed for the specimen tested at the constant high stress amplitude of 1100 MPa [2], the relative smooth area between the fine granular areas in the "tree-ring" feature was due to the crack propagation under the high stress amplitude of 1100 MPa. It indicated that the high loading accelerated the crack growth or damage development compared with the constant target amplitude loading, and shortened the fatigue life.

It was noted that the effect of high loading on the VHCF behavior was also related to the loading sequence, loading cycles and stress level. For example, the specimens of the martensitic stainless steel (AISI630) failed from both the surface and the interior under the constant high stress amplitude and failed from only the interior of the specimen with FGA characteristic under the constant low stress amplitude ($\leq$473 MPa) [21]. While the specimen could fail from the surface inclusion without FGA feature under the variable amplitude loading with a block of low stress amplitude of 450 MPa for 2×10^6 cycles and followed by a block of high stress amplitude of 650 MPa for 4×10^3 cycles, as shown in Fig. 12. This indicated that an introduction of high loading in variable amplitude loading could not only reduce the VHCF life in terms of the target loading but also change the fatigue failure mechanism to the one dominated by the high loading.

4. Conclusion

The effects of natural aging and variable loading on VHCF behavior of GCr15 steel have been investigated by ultrasonic frequency fatigue tests. SEM observation indicated that fatigue cracks of all the failed specimens initiated from the interior of the specimens. The main conclusions of this study are as follows:

- A natural aging of 10000 h prolonged the fatigue life of GCr15 steel in VHCF regime. It was attributed to that more granular carbides precipitated in the microstructure after natural aging, and they could strengthen the material as well as restrain the crack initiation and growth. The natural aging had no obvious influence on the characteristics of crack initiation and early growth of the GCr15 steel in VHCF regime.
- The effect of low loading in variable amplitude loadings on the VHCF life in terms of target stress amplitude was related to the loading sequence, loading cycles and stress level. Once the crack or damage formed by the target stress amplitude was large enough in the crack initiation and early growth stage, the subsequent low loading could promote the crack growth or damage development, and finally reduced the VHCF life. The low loading had no influence on the characteristics of crack initiation and early growth of GCr15 steel in VHCF regime.
- The high loading with a small number of cycles in variable amplitude loading could accelerate the crack initiation and growth, and reduced the VHCF life in terms of the target stress amplitude. It could also change the fatigue failure mechanism dominated by the target stress amplitude.

Data availability.

The data are available upon request by contacting with the corresponding author.

CRediT authorship contribution statement

Gen Li: Methodology, Investigation, Writing – review & editing, Funding acquisition. **Lei Ke:** Investigation, Writing – review & editing. **Wenjie Peng:** Investigation, Writing – review & editing. **Xuechong Ren:** Investigation, Writing – review & editing. **Chengqi Sun:** Conceptualization, Methodology, Investigation, Writing – review & editing, Funding acquisition, Supervision.

Declaration of Competing Interest

The authors declare that they have no known competing financial interests or personal relationships that could have appeared to influence the work reported in this paper.

Acknowledgements

The authors gratefully acknowledge the support of the National Natural Science of China Basic Science Center for "Multiscale Problems in Nonlinear Mechanics" (11988102) and the fund of International Postdoctoral Exchange Fellowship Program (China).

References

[1] C. Sun, Q. Song, L. Zhou, J. Liu, Y. Wang, X. Wu, Y. Wei, The formation of discontinuous gradient regimes during crack initiation in high strength steels under very high cycle fatigue, Int. J. Fatigue 124 (2019) 483–492, https://doi.org/10.1016/j.ijfatigue.2019.03.026.
[2] Q. Song, C. Sun, Mechanism of crack initiation and early growth of high strength steels in very high cycle fatigue regime, Mater. Sci. Eng., A 771 (2020) 138648, https://doi.org/10.1016/j.msea.2019.138648.
[3] Z. Huang, D. Wagner, C. Bathias, P. Paris, Subsurface crack initiation and propagation mechanisms in gigacycle fatigue, Acta Mater. 58 (18) (2010) 6046–6054, https://doi.org/10.1016/j.actamat.2010.07.022.
[4] B. Nie, Z. Zhao, Y. Ouyang, D. Chen, H. Chen, H. Sun, S. Liu, Effect of low cycle fatigue predamage on very high cycle fatigue behavior of TC21 titanium alloy, Materials 10 (12) (2017) 1384, https://doi.org/10.3390/ma10121384.
[5] X. Wang, E. Feng, C. Jiang, A microplasticity evaluation method in very high cycle fatigue, Int. J. Fatigue 94 (2017) 6–15, https://doi.org/10.1016/j.ijfatigue.2016.09.004.
[6] A. Zhao, J. Xie, C. Sun, Z. Lei, Y. Hong, Effects of strength level and loading frequency on very-high-cycle fatigue behavior for a bearing steel, Int. J. Fatigue 38 (2012) 46–56, https://doi.org/10.1016/j.ijfatigue.2011.11.014.
[7] W. Li, T. Sakai, Q. Li, L. Lu, P. Wang, Reliability evaluation on very high cycle fatigue property of GCr15 bearing steel, Int. J. Fatigue 32 (7) (2010) 1096–1107, https://doi.org/10.1016/j.ijfatigue.2009.12.008.
[8] K. Shiozawa, T. Hasegawa, Y. Kashiwagi, L. Lu, Very high cycle fatigue properties of bearing steel under axial loading condition, Int. J. Fatigue 31 (5) (2009) 880–888, https://doi.org/10.1016/j.ijfatigue.2008.11.001.
[9] T. Sakai, Review and prospects for current studies on very high cycle fatigue of metallic materials for machine structural use, J. Solid Mech. Mater. Eng. 3 (3) (2009) 425–439, https://doi.org/10.1299/jmmp.3.425.
[10] L. Botvina, I. Petrova, I. Gadolina, V. Levin, Y. Demina, A. Soldatenkov, M. T'utin, High-cycle fatigue failure of low-carbon steel after long-term aging, Inorganic Materials, 2010. 46(14): p. 1570-1577. https://doi.org/10.1134/S0020168510140190.
[11] P. Chang, Temper-aging of continuously annealed low carbon dual phase steel, Metall. Trans. A 15 (1) (1984) 73–86, https://doi.org/10.1007/BF02644389.
[12] M. Zamani, H. Mirzadeh, M. Maleki, Enhancement of mechanical properties of low carbon dual phase steel via natural aging, Mater. Sci. Eng., A 734 (2018) 178–183, https://doi.org/10.1016/j.msea.2018.07.105.
[13] M. Sander, T. Muller, J. Lebahn, Influence of mean stress and variable amplitude loading on the fatigue behaviour of a high-strength steel in VHCF regime, Int. J. Fatigue 62 (2014) 10–20, https://doi.org/10.1016/j.ijfatigue.2013.04.015.
[14] M. Sander, T. Muller, C. Stacker, Very high cycle fatigue behavior under constant and variable amplitude loading, Procedia Struct. Integrity 2 (2016) 34–41, https://doi.org/10.1016/j.prostr.2016.06.005.
[15] H. Mayer, W. Haydn, R. Schuller, S. Issler, M. Bacher-Hochst, Very high cycle fatigue properties of bainitic high carbon–chromium steel under variable amplitude conditions, Int. J. Fatigue 31 (8–9) (2009) 1300–1308, https://doi.org/10.1016/j.ijfatigue.2009.02.038.
[16] H. Mayer, Fatigue damage of low amplitude cycles in low carbon steel, J. Mater. Sci. 44 (18) (2009) 4919–4929, https://doi.org/10.1007/s10853-009-3751-x.
[17] C. Sun, Q. Song, Y. Hu, Y. Wei, Effects of intermittent loading on fatigue life of a high strength steel in very high cycle fatigue regime, Int. J. Fatigue 117 (2018) 9–12, https://doi.org/10.1016/j.ijfatigue.2018.07.033.
[18] W. Peng, Y. Zhang, B. Qiu, H. Xue, A brief review of the application and problems in ultrasonic fatigue testing, AASRI Procedia 2 (2012) 127–133, https://doi.org/10.1016/j.aasri.2012.09.024.
[19] W. Peng, S. Wu, H. Xue, Z. Peng, D. Liu, Measurement approach of dynamic strain and stress calibration for ultrasonic fatigue specimens, Mech. Sci. Technol. Aerospace Eng. (2021), https://doi.org/10.13433/j.cnki.1003-8728.20200606.
[20] M. Ijaz, F. Qayyum, H. Elahi, M. Ullah, Effect of natural aging and fatigue crack propagation rate on welded and non-welded aluminum alloy (AA2219-T87), Adv. Sci. Technol. Res. J. 13 (3) (2019), https://doi.org/10.12913/22998624/110737.
[21] C. Sun, Q. Song, L. Zhou, X. Pan, Characteristic of interior crack initiation and early growth for high cycle and very high cycle fatigue of a martensitic stainless steel, Mater. Sci. Eng., A 758 (2019) 112–120, https://doi.org/10.1016/j.msea.2019.04.015.

[22] C. Sun, Q. Song, A method for predicting the effects of specimen geometry and loading condition on fatigue strength, Metals 8 (10) (2018) 811, https://doi.org/10.3390/met8100811.
[23] Y. Akiniwa, N. Miyamoto, H. Tsuru, K. Tanaka, Notch effect on fatigue strength reduction of bearing steel in the very high cycle regime, Int. J. Fatigue 28 (11) (2006) 1555–1565, https://doi.org/10.1016/j.ijfatigue.2005.04.017.
[24] Y. Murakami, Analysis of stress intensity factors of modes I, II and III for inclined surface cracks of arbitrary shape, Eng. Fract. Mech. 22 (1) (1985) 101–114, https://doi.org/10.1016/0013-7944(85)90163-8.
[25] A. Zhao, J. Xie, C. Sun, Z. Lei, Y. Hong, Prediction of threshold value for FGA formation, Mater. Sci. Eng., A 528 (22–23) (2011) 6872–6877, https://doi.org/10.1016/j.msea.2011.05.070.
[26] K. Shiozawa, L. Lu, S. Ishihara, S-N curve characteristics and subsurface crack initiation behaviour in ultra-long life fatigue of a high carbon-chromium bearing steel, Fatigue Fract. Eng. Mater. Struct. 24 (12) (2001) 781–790, https://doi.org/10.1046/j.1460-2695.2001.00459.x.
[27] S. Kalnaus, F. Fan, A. Vasudevan, Y. Jiang, An experimental investigation on fatigue crack growth of AL6XN stainless steel, Eng. Fract. Mech. 75 (8) (2008) 2002–2019, https://doi.org/10.1016/j.engfracmech.2007.11.002.
[28] S. Li, Y. Zhang, L. Qi, Y. Kang, Effect of single tensile overload on fatigue crack growth behavior in DP780 dual phase steel, Int. J. Fatigue 106 (2018) 49–55, https://doi.org/10.1016/j.ijfatigue.2017.09.018.
[29] P. Lopez-Crespo, A. Steuwer, T. Buslaps, Y.H. Tai, A. Lopez-Moreno, J.R. Yates, P. J. Withers, Measuring overload effects during fatigue crack growth in bainitic steel by synchrotron X-ray diffraction, Int. J. Fatigue 71 (2015) 11–16, https://doi.org/10.1016/j.ijfatigue.2014.03.015.
[30] Y. Hong, Z. Lei, C. Sun, A. Zhao, Propensities of crack interior initiation and early growth for very-high-cycle fatigue of high strength steels, Int. J. Fatigue 58 (2014) 144–151, https://doi.org/10.1016/j.ijfatigue.2013.02.023.
[31] K. Shiozawa, Y. Morii, S. Nishino, L. Lu, Subsurface crack initiation and propagation mechanism in high-strength steel in a very high cycle fatigue regime, Int. J. Fatigue 28 (11) (2006) 1521–1532, https://doi.org/10.1016/j.ijfatigue.2005.08.015.
[32] Q. Wang, C. Bathias, N. Kawagoishi, Q. Chen, Effect of inclusion on subsurface crack initiation and gigacycle fatigue strength, Int. J. Fatigue 24 (12) (2002) 1269–1274, https://doi.org/10.1016/S0142-1123(02)00037-3.
[33] X. Lu, S. Zheng, Strengthening and damaging under low-amplitude loads below the fatigue limit, Int. J. Fatigue 31 (2) (2009) 341–345, https://doi.org/10.1016/j.ijfatigue.2008.08.004.
[34] S. Zheng, H. Xu, J. Feng, Z. Zheng, Y. Wang, L. Lu, Lightweight design of automobile drive shaft based on the characteristics of low amplitude load strengthening, Chin. J. Mech. Eng. 24 (6) (2011) 1111, https://doi.org/10.3901/CJME.2011.06.1111.
[35] S. Zheng, G. Liang, Z. Wang, J. Feng, Z. Ma, Compilation of automotive lower control arm spectrum based on the low-amplitude training load, J. Mech. Eng. 50 (16) (2014) 147–154. http://www.cjmenet.com.cn/CN/Y2014/V50/I16/147.
[36] G. Sinclair, An investigation of the coaxing effect in fatigue of metals. 1952, ILLINOIS UNIV AT URBANA.